

Formation of Non-Equilibrium Alloys by High Pressure Melt Quenching[†]

Z. Q. Hu^{*} B. Z. Ding H. F. Zhang D. J. Li B. Yao
H. Z. Liu A. M. Wang

State Key Laboratory of Rapidly Solidified Non-equilibrium Alloys, Institute of Metal Research,
Chinese Academy of Sciences, Shenyang 110016, People's Republic of China

Abstract: Melt quenching under high pressure can promote the formation of metastable materials. High pressure accelerates the amorphization of $\text{Cu}_{60}\text{Ti}_{40}$ and $\text{Cd}_{43}\text{Sb}_{57}$. For an alloy system having volume expansion after solidification, the higher the applied pressure, the lower the melting point and the higher the amorphization temperature, which promotes the formation of metallic glass. High pressure also enhances nucleation and suppresses grain growth, so solidification under high pressure can refine the crystal grains to form nanocrystalline alloys, such as $\text{Ti}_{60}\text{Cu}_{40}$, $\text{Cu}_{70}\text{Si}_{30}$ and $\text{Pd}_{78}\text{Si}_{16}\text{Cu}_6$ alloys. ©2001 Elsevier Science Ltd. All rights reserved.

Key Words: Non-equilibrium alloys; High pressure melt quenching; Amorphous alloys; Nanocrystalline alloys

1 Introduction

Much research has been done on solid-state amorphization under high pressure, for example, graphite transforms to amorphous state at 293K when the pressure exceeds 20GPa^[1]; when pressure is applied, semiconductor Ge and Si change to conductor, but they transform to the amorphous state after the pressure is removed^[2,3]. It is also reported that amorphization occurs in Cd-Sb^[4],

[†] 原文原载于《Science and technology of Advanced Materials》, 2001, 2: 41~48.

^{*} Corresponding author.

E-mail address: zqhu@imr.ac.cn(Z.Q.Hu).

1468-6996/01/\$ -see front matter ©2001 Elsevier Science Ltd. All rights reserved.

PII: S 1468-6996(01)00024-9

Zn-Sb^[5], Ga-Sb^[6] and Al-Ge^[7] alloy systems. Amorphization forms more easily by high pressure melt quenching than by solid-state reaction. Minomura et al.^[8] prepared integrated semiconductor bulk metallic glass by melting GaSb under 3~10GPa, then cooling to room temperature under pressure. Xu et al.^[9] prepared Pd₄₀Ni₄₀P₂₀ bulk amorphous material by means of the pressure melt quenching method, i.e. keeping the pressure and temperature at 5.5GPa and 1200K (300K higher than the melting point of the alloy) for 1~2h, then cooling to room temperature at a rate of 200K/s. Mao et al.^[10] acquired bulk Zr₆₀Ni₂₀Al₂₀ amorphous alloy with crystallization temperature at 755K by the same method. Other metastable phases can also be prepared by the pressure melt quenching method, e.g. Su et al.^[11] prepared Al-Mn, Al-Mn-Si quasicrystalline materials by this method. Popova et al.^[12] reported that they prepared Cu₈₅Sn₁₅ amorphous alloy by melting the alloy under high pressure, cooling to room temperature at a cooling rate of 10³ K/s, then releasing the pressure, the size of the amorphous bulk achieving millimeter scale. In general, it is the high pressure that suppresses the diffusion process and lowers the critical cooling rate of the amorphous formation, so metallic glass can be formed at a relatively lower cooling rate. Brixner^[13] tried to make Gd₂(MoO₄)₃ transform from low-density metastable β and β' phases to high density stable α phase by high pressure. The sample was pressurized to 6.5GPa, kept for 2h at various temperatures under pressure and then cooled. In the temperature range from 200 °C to 400 °C, Gd₂(MoO₄)₃ transformed to an amorphous phase (π phase) after heat and pressure treatment. The low density metastable β and β' phases tended to transform to α phase at above 500°C under pressure. However, at low temperature, the intermediate disorder phase was frozen in an amorphous state because of the poor kinetics. A structural change with large volume effect always undergoes the amorphous state.

In high pressure phase transformation, materials always change from a low density to a high density phase. Thus the crystal-crystal and amorphous-crystal transition under pressure are easy to be understood. However, in the research of high pressure phase transformation, especially in recent years, it was found that solid crystalline materials could turn to the amorphous state under high pressure, called pressure induced solid state amorphization. It was also found that under high pressure, bulk amorphous material could be acquired by means of quenching the melt at a cooling rate much lower than that under atmospheric pressure, which

became an effective method for preparing bulk amorphous material.

As discussed earlier, because the original discovery was accidental, it did not attract many attentions. Along with the research and development of high pressure technology, many similar experimental phenomena were found not only in alloys, but also in many elements and compounds. Thus this kind of phenomenon is universal. Not only amorphous, but also nanocrystalline materials and nanocomposites can be prepared through the non-equilibrium process of quenching the melt under high pressure. To study the laws and mechanisms of the solidification process of melt under high pressure is significant from both academic and practical aspects.

2 Experimental Procedure

The high pressure equipment used in the present experiment was a belt-type apparatus re-equipped by the authors. It consists mainly of pressure generating, heating and temperature controlling items, as well as measuring instruments. It can generate pressure of up to 9GPa and temperatures of up to 1800K with a precision of 0.2%. The pressure was previously calibrated by measuring the phase transition point of Bi and Ba under pressure at room temperature. The size of the samples was ϕ 3mm \times 3mm. The high pressure apparatus is illustrated in Fig. 1.

In the experiment, the sample was put into a BN crucible which was inserted in a graphite heater, pressed to a desired pressure, kept at pressure for 5~10min to make the pressure well-distributed and steady in the pressure cell, then heated to the desired temperature at various heating rates under pressure. After keeping the temperature and pressure for a desired time period, and then the sample was rapidly cooled down to room temperature at a cooling rate of up to 300K/s, by switching off the heater, because the heat of the sample was transmitted rapidly through the WC anvils cooled by water.

The structure and phase analyses were examined using DSC, XRD, SEM and TEM.

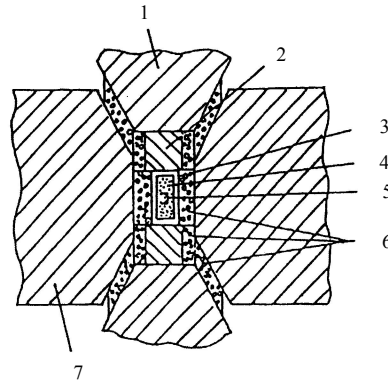


Fig. 1 Schematic map of the belt-type high pressure apparatus

1—WC anvil; 2—WC piston; 3—graphite heater; 4—BN crucible; 5—sample; 6—pyrophyllite; 7—
WC ring

3 Experimental Results

3.1 Amorphous Alloy

Since amorphous alloy was first discovered, many efforts have been made to prepare large bulk amorphous alloy with outstanding properties and these have been well-used in practice. One kind of method is increasing the energy of crystal to make it transform spontaneously into the amorphous state at low temperature (lower than the crystallization temperature of the corresponding amorphous alloy). A typical example is solid state reaction amorphization under high pressure. High pressure results in the formation of a new metastable phase with energy higher than the amorphous state, which can decompose to form amorphous material spontaneously at room temperature. Another method is trying to freeze the disordered state (e.g. the liquid state), such as vapour deposition, melt spinning, etc. The starting point of predecessors is to make the time insufficient for atoms to move, so that long range diffusion cannot occur. However, this class of method cannot secure a large bulk of amorphous material because it needs an ultrarapid cooling rate. High pressure is a very effective method for this purpose. Owing to the introduction of pressure, the distance between atoms decreases, and atoms are difficult to diffuse, so that the entire disordered state is retained more easily to form a large bulk amorphous alloy.

The formation of Cu-Ti amorphous alloy was investigated by Li et al. The result of X-ray diffraction analysis showed that $\text{Cu}_{60}\text{Ti}_{40}$ transformed to amorphous material after cooling under 5.5 GPa from 1573K with a cooling rate of 300K/s. The electron diffraction image of amorphous $\text{Cu}_{60}\text{Ti}_{40}$ was clearly an amorphous

ring, as shown in Fig. 2^[14]. When a $\text{Cu}_{60}\text{Ti}_{40}$ sample was cooled under 5.5GPa from 1573K with cooling rate of 50K/s, there was still a weak amorphous peak in the XRD spectrum. These results show that under the same pressure, the more rapid is the cooling rate, the easier it is for the high temperature disordered state to be retained. When the $\text{Cu}_{60}\text{Ti}_{40}$ sample was cooled under 5.5GPa from 1373K with cooling rate of 300K/s after retaining the pressure and temperature for 5min, partially amorphous material with an obviously diffused amorphous peak was gained. However, the sample quenched under 3GPa from 1473K with 300K/s was an entirely crystalline phase from XRD analysis. These results show there is a critical pressure in pressure melt quenching, if the pressure is lower than the critical value, amorphous phase cannot form. For $\text{Cu}_{60}\text{Ti}_{40}$ alloy, when the cooling rate was 300K/s, the critical pressure was in the range of 3~4GPa.

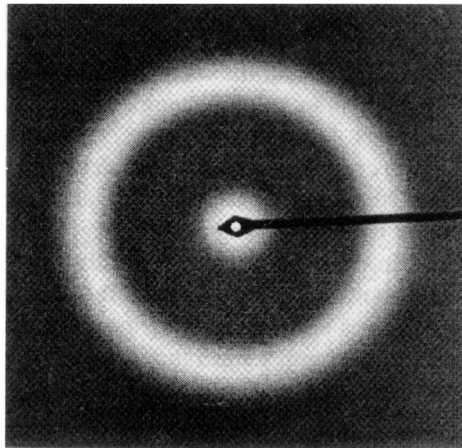


Fig. 2 Electron diffraction pattern of amorphous Cu-Ti ^[14]

It was confirmed that amorphous alloy could also be acquired by quenching melt under pressure in the Cd-Sb system, as shown in Fig. 3^[14-17]. Under 8 GPa, the sample was heated to 623K, kept at the temperature for 5min, then quenched in a liquid nitrogen temperature at a rate of about 10^2 K/s. Fig.3(a) shows the XRD curve of the original crystalline $\text{Cd}_{43}\text{Sb}_{57}$ alloy, whilst Fig.3(b)~(f) show the high pressure metastable phase of the sample kept at room temperature after pressure release for 12h, 24h, 36h, 48h and 60h, respectively. The metastable phase after quenching under pressure, called the γ phase, was a simple hexagonal structure with $a = 0.3182$ nm and $c = 0.2939$ nm. γ metastable phase gradually disappeared with time, as shown in Fig. 3(b)~(e). It transformed completely to amorphous phase after 60h, as shown in Fig.3(f). Fig.4 shows the thermoanalysis curve of the amorphous alloy. There is an exothermal peak, i.e. the crystallization peak of the

amorphous, which appeared at 385K, and an endothermic peak at 727K with a new unknown phase formed.

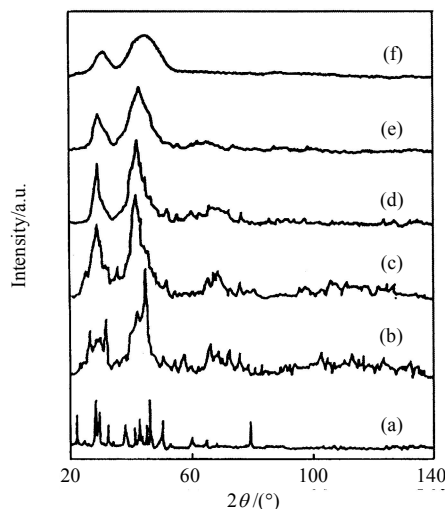


Fig. 3 Cd-Sb Amorphous alloy prepared by the pressure-quenching method.

(a) is original crystalline sample; (b)~(f) are high pressure metastable phase kept at room temperature for 12h, 24h, 36h, 48h and 60h, respectively

3.2 Nanocrystalline Materials

In general, the process of preparing nanocrystalline materials is how to control the nucleation and growth of the material. In order to acquire nanometer-scaled crystals, the nucleation rate must be increased and the growth rate depressed. Because of the effect of pressure on the activation energy of viscous flow and melting temperature, the nucleation rate increases and growth rate decreases in a certain pressure range.

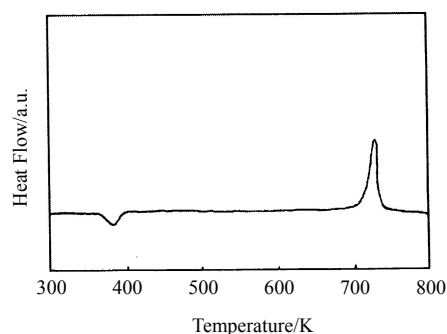


Fig. 4 DSC result of crystallization of Cd-Sb amorphous sample (The exothermic peak is at 385K, and the endothermic peak, 727K. The heating rate is 5K/min)

Owing to the influence of pressure on the nucleation and growth rate, bulk nanocrystalline materials can be obtained under low cooling rate, and the grain size can be controlled by adjusting the pressure. The nanocrystals are formed

directly from the solidification of the melt, the entire process being performed in a hermetically sealed high pressure cell, and the cooling rate is low, so the prepared bulk nanocrystalline materials have clear interfaces and relatively higher density. For an example, nanocrystalline Zn with grain size of 20 nm can be prepared by this method^[18].

The preparation and structure of Pd–Si–Cu nanocrystalline alloy were investigated^[19]. Pd₇₈Si₁₆Cu₆ master alloy was prepared by smelting the mixture of Pd(99.999%), Si(99.99%) and Cu(99.99%) powders in a vacuum arc furnace under the protection of argon atmosphere, its XRD spectrum being shown in Fig. 5. The master alloy was placed into a boron nitride (BN) crucible, which was encased within a graphite heater, and pressed to the desired pressure. Then it was heated to 1300K for 20min under the pressure to make the Pd₇₈Si₁₆Cu₆ master alloy melt fully to decrease the number of atom clusters in the liquid. After the power was switched off to stop heating, since both ends of the BN crucible were in close contact with tungsten carbide (WC) anvils cooled by water, and the crucible itself had good thermal conductivity, the sample was cooled down rapidly at a rate of 200K/s. Fig. 5(b)~(e) show the XRD spectra of the Pd₇₈Si₁₆Cu₆ alloy samples quenched from 1300K under pressures of 2GPa, 4GPa, 5GPa and 6GPa, respectively. The sample was composed of fcc Pd(Cu) solid solution and metastable phase-II Pd₄Si. It was calculated that the lattice constant of fcc Pd(Cu) solid solution was $a = 0.3854\text{nm}$. Using the Vegard law, it was evaluated that the solid solubility of copper in palladium was approximately 15%. As shown in Fig. 5, the widths of XRD peaks of both fcc Pd(Cu) and metastable phase-II Pd₄Si broadened with increasing pressure. By

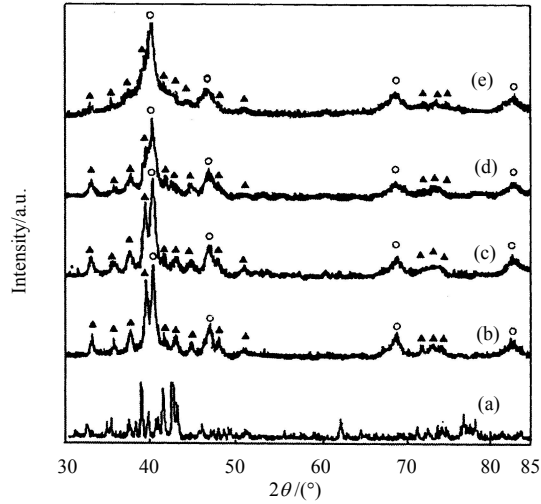


Fig. 5 XRD spectra of Pd₇₈Si₁₆Cu₆ master alloy (a) and the sample prepared by melt-quenching from 1300K under 2 GPa (b), 4 GPa (c), 5 GPa (d) and 6 GPa (e)^[19]

○ Pd(Cu); ▲ Pd₄Si-II

means of the half-peak width of the XRD lines, the grain size, d , could be calculated using the Scherrer equation:

$$d = \frac{0.89\lambda}{\beta \cos\theta} \quad (1)$$

where $\lambda = 0.15405\text{nm}$ was the X-ray wavelength, θ the Bragg angle, and β the pure half-peak width excluding the width resulting from instrument broadening. The mean grain sizes of fcc Pd(Cu) and metastable phase-II Pd₄Si were calculated and listed in Table 1. According to the above experimental results and analysis, it is concluded that a Pd-Si-Cu bulk nanocrystalline material can be prepared by the high pressure melt quenching method, where the higher the pressure, the smaller the grain size.

Table 1 Mean grain sizes of pressure-quenched Pd-Si-Cu samples

Pressure/GPa	Pd(Cu) solid solution/nm	Pd ₄ Si-II/nm
2	11.6	36
4	9.0	25
5	8.4	17
6	8.0	13

When Ti₆₀Cu₄₀ alloy was quenched from 1500K under a pressure of 1~6GPa at a cooling rate of 200 K/s, grains with sizes of 7.3~13.3nm were formed, as shown in Fig. 6^[20,21].

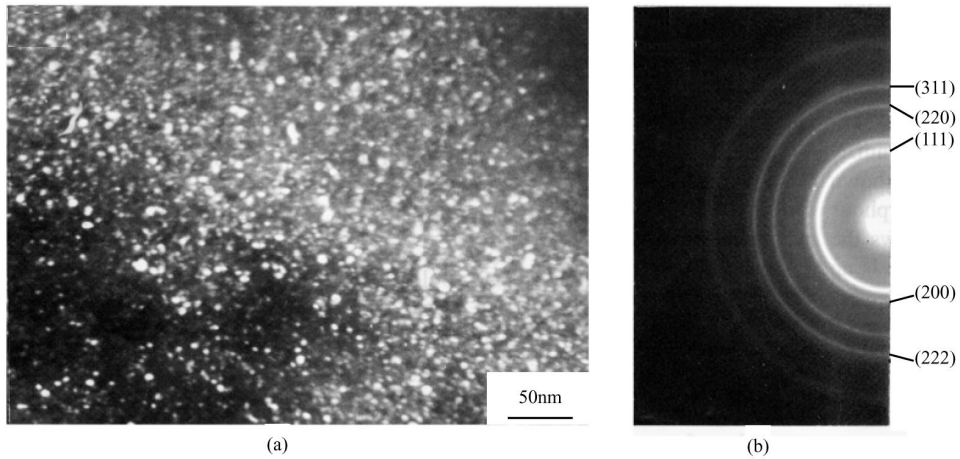


Fig. 6 TEM images of the $\text{Ti}_{60}\text{Cu}_{40}$ sample quenched from 1500K at 200K/s under 4 GPa

(a) bright field image; (b) electron diffraction pattern

$\text{Cu}_{70}\text{Si}_{30}$ alloy was heated at 1300K under 6GPa pressure for 10min, then quenched from melt to room temperature at a rate of 200K/s. It was established by XRD and electron diffraction that the quenched alloy consisted of γ' - Cu_5Si and metastable phase C, and their grain sizes were 20nm and 17nm, respectively, as shown in Fig. 7. The C phase transformed to η (Cu,Si) phase after annealing^[22].

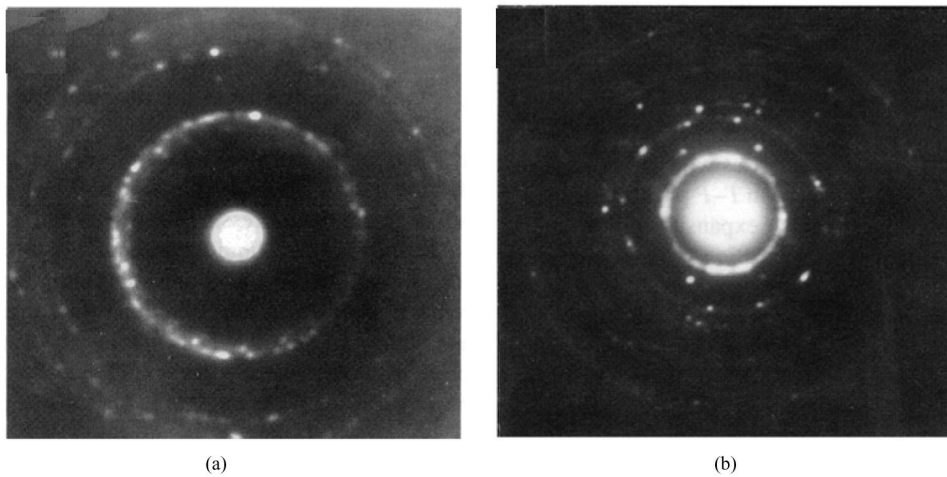


Fig. 7 Electron diffraction patterns of $\text{Cu}_{70}\text{Si}_{30}$ nanocrystalline alloy

(a) γ - Cu_5Si ; (b) C (Cu, Si)

3.3 Nanocomposite

Nickel powder (99.99%) and aluminium powder (99.99%) were mixed uniformly with a molar ratio of 20:1. The mixture was put into a BN cell, then heated to 1073~1473K under high pressure with a heating rate of 450K/min. After keeping under high pressure and high temperature conditions for 10min, the sample was quenched under high pressure to room temperature with a cooling rate of

200~300K/s. Fig.8 shows the TEM images of Al_3Ni whiskers inlaid into Al matrix which were synthesized under 1273K and 4GPa condition^[23]. The composition of point A in Fig. 8 was 75.2%Al and 24.8%Ni by EDAX. The Al_3Ni whiskers were 80 nm in diameter and 1~2 μm in length. The density of the nanocomposite was 2.86g/cm³. Fig.9 shows the influence of pressure on the microhardness of $\text{Al}_3\text{Ni}_w/\text{Al}$ nanocomposite.

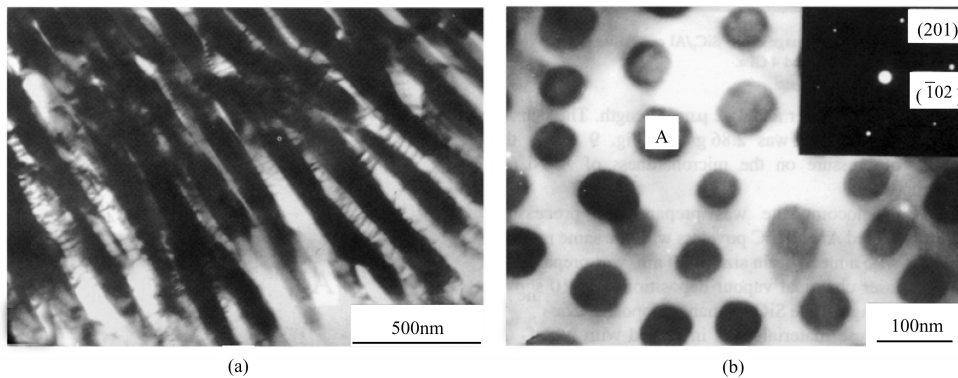


Fig. 8 TEM morphologies of the $\text{Al}_3\text{Ni}_w/\text{Al}$ nanocomposite synthesized at 1273K and 4GPa
 (a) typical morphology of the Al_3Ni whiskers formed in the Al matrix; (b) bright field TEM image of a transverse section of Al_3Ni whiskers in the Al matrix, together with the corresponding electron diffraction patterns

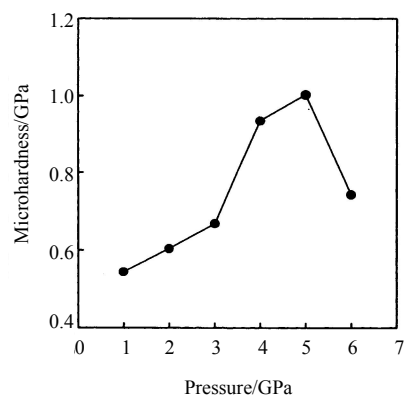


Fig. 9 Microhardness of $\text{Al}_3\text{Ni}_w/\text{Al}$ Nanocomposites Synthesized at 1273 K as a Function of Pressure

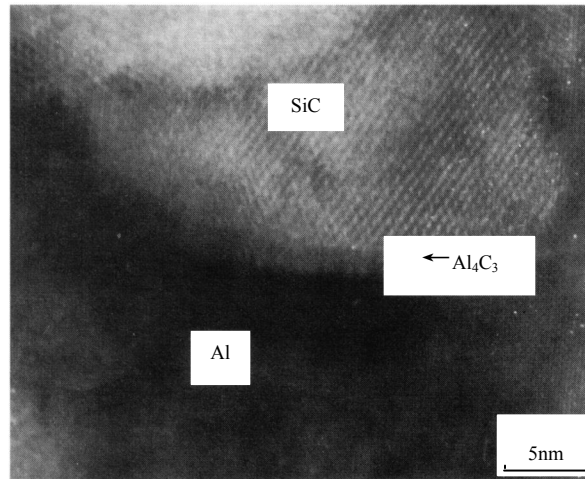


Fig. 10 A typical HREM image of the SiC_p/Al composite (SiC 20 vol%) synthesized under 1073 K and 4 GPa

SiC_p/Al nanocomposite was prepared by processing uniformly mixed Al and SiC powders with the same method^[24]. SiC, with a mean grain size of 30nm, was prepared by means of laser chemical vapour deposition. Fig.10 shows the HREM image of the SiC_p/Al nanocomposite. The microhardness of these materials was increased with increasing temperature and content of SiC, as shown in Fig. 11.

4 Discussion

4.1 Influence of Pressure on the Formation of Amorphous Alloy

Pressure has influences on the viscosity and density of liquid^[25]. If the viscosity of liquid under normal pressure is η_0 , its viscosity $\eta(P)$ under pressure P can be expressed as:

$$\eta(P) = \eta_0 \exp[(E + PVN)/kT] \quad (2)$$

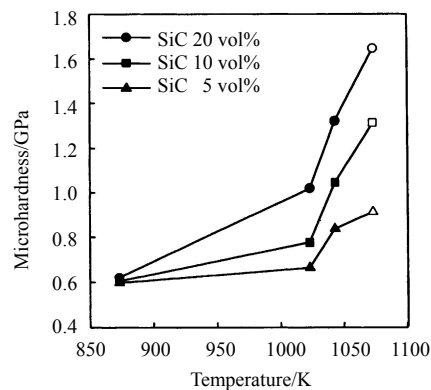


Fig. 11 The Microhardness of SiC_p/Al composite synthesized under 4 GPa at various temperatures and for three different fractions of SiC particles

where E is the activation energy for viscous flow, V is the volume, N is the Avogadro number, k is the Boltzmann constant, and T is the absolute temperature. The viscosity of liquid increases with increasing pressure. The viscosity of solid also increases with pressure, but the volume change of solid is less than that of liquid. Although the viscosity of solid under normal pressure is far higher than that of liquid, the increment of the viscosity of liquid with pressure is much faster than that of solid. Thus there is an intersection point between the curves of viscosity of liquid and solid with pressure, and the pressure here is the critical pressure P_c .

At the same time a similar relation exists between the density of liquid and solid. Under normal pressure, the density of liquid is less than that of solid. When the pressure rises, the density of liquid increases, but the rate of density increase of liquid is much faster than that of solid. When the melting temperature decreases with increasing pressure, i.e. the slope of melting curve in T - P phase diagram is negative, solidification is a volume expansion process, so that pressure will suppress the transition from liquid to the original crystalline state, and promote the conservation of the disordered liquid state at room temperature. The condition for amorphous formation by the high pressure melt quenching method is a system with negative slope on the melting curve. The melting temperature increases with decreasing pressure only when pressure is higher than the critical value, so that the amorphous formation ability depends on the value of the critical pressure. A system with higher compression ratio has a smaller critical pressure, and amorphous material can form more easily.

The glass forming temperature T_g under high pressure is also in relation to pressure^[26]:

$$T_g = T_g^* (E + W + PVN) / (E^* + W^*) \quad (3)$$

where T_g^* is the glass forming temperature under normal pressure, W^* is the potential barrier for nucleation under normal pressure, and W is the barrier potential under pressure P . From Eq.(3), it can be concluded qualitatively that T_g increases with increasing pressure for $W^* \ll E^*$.

(1) For a system with $\Delta V_f = V_L - V_S > 0$, $dT_m/dP > 0$, the melting point T_m

increases with pressure P , so that although T_g increases with pressure, the criterion for the ability of amorphous formation, T_g/T_m , varies slightly with pressure.

(2) For a system with $\Delta V_f = V_L - V_S < 0$, $dT_m/dP < 0$, the melting point T_m decreases with pressure P , but T_g still increases with pressure. The combination of the two reasons result in the increase of T_g/T_m , so that the amorphous forming ability increases.

From the above analyses, it can be concluded that a system with $\Delta V_f = V_L - V_S < 0$ could form amorphous by means of quenching the melt under pressure, i.e. pressure is favorable to the formation of amorphous material, and the higher the $|\Delta V_f|$, the lower the pressure needed, and the easier the amorphous formation.

4.2 Influence of Pressure on the Formation of Nanocrystalline Materials

Based on the classical theory of homogeneous nucleation, and neglecting the influence of pressure on the surface energy, the influence of pressure on the nucleation rate can be derived:

$$\frac{I(P)}{I(P_0)} = \exp \frac{\Delta G^I(P_0) - \Delta G^I(P)}{RT} \quad (4)$$

where $I(P)$ is the nucleation rate under high pressure, $I(P_0)$ the nucleation rate under normal pressure, $\Delta G^I(P)$ the nucleation activation energy under high pressure, $\Delta G^I(P_0)$ the nucleation activation under normal pressure, P the pressure and T the absolute temperature. In general, when pressure increases, the nucleation energy decreases, so that $I(P) > I(P_0)$.

Diffusion of atoms is necessary for the growth of grains, i.e. the grain growth activation is in relation to the diffusion activation energy. The change of diffusion coefficient D with pressure can be expressed as:

$$\frac{\partial \ln D}{\partial P} = -\frac{1}{RT} \frac{\partial \Delta G}{\partial P} = -\frac{\Delta V^*}{RT} \quad (5)$$

where ΔG is diffusion activation energy, and ΔV^* the activation volume. Because $\Delta V^* > 0$, the diffusion energy increases and the diffusion coefficient decreases with pressure, i.e. pressure depresses diffusion. Thus it can be deduced that $U(P) < U(P_0)$, where $U(P)$ and $U(P_0)$ are the growth rate of grains under high pressure and normal pressure, respectively.

The mean grain size can be expressed as follows:

$$d = \left(\frac{U}{I} \right)^{1/4} \quad (6)$$

The influence of pressure on grain size can be expressed as:

$$\frac{d(P)}{d(P_0)} = \left[\frac{U(P)}{U(P_0)} \right]^{1/4} \left[\frac{I(P_0)}{I(P)} \right]^{1/4} \quad (7)$$

From the above analyses, it is concluded that pressure promotes nucleation but suppresses grain growth, so solidification under high pressure can refine the grain size, which is the same as is found in experimental results.

5 Conclusions

(1) For an alloy system with $\Delta V_f = V_L - V_S < 0$, pressure promotes the amorphous formation by quenching from melt.

(2) Pressure accelerates nucleation and decelerates grain growth. Solidification under high pressure promotes the grain refinement.

(3) The amorphous alloy, nanocrystalline alloys and nanocomposite prepared by high pressure melt quenching have high density and clear interfaces. By using this method, one can acquire bulk amorphous materials at much lower cooling rate than under normal pressure, or some high pressure metastable materials that is difficult to be prepared under normal pressure.

Acknowledgements

This project was supported by the National Natural Science Foundation of China.

References

- [1] Goncharov A F. JETP Lett. 1990, 51: 418
- [2] Shinomura O, Minomura S, Sakai N, Asumi K, Tamuro K, Fukushima J, Endo E. Phil. Mag., 1974, 29: 547
- [3] Chang K J, Dacorona M M, Cohen M L. Phys. Rev. Lett., 1985, 54: 2375
- [4] Belash I T, Ponyatovsky E G. High Temp. High Press, 1974, 6: 241
- [5] Aprekar I T, Belash I T, Ponyatovsky E G. High Temp. High Press, 1977, 9: 641
- [6] McDonald T R R, Sard R, Gregory E. Science, 1965, 147: 1441
- [7] Barkalov O I, Belash I T, Degtyareva V F, Ponyatovsky E G. Sov. Phys. Solid State, 1987, 29: 1138
- [8] Minomura S, Shimonura O, Asami K, Oyanagi H, Takemura K. In: Spear W E. Proceedings of the

- [9] Xu Y F, Huang X M, Wang W K. Appl. Phys. Lett., 1990, 56: 1957
- [10] Mao Z L, Chen H, Wang W K. J. Mater. Sci. Lett., 1993, 12: 1729
- [11] Yao B, Zhang Q, Su W H. Chin. J. High Press. Phys., 1990, 4: 50
- [12] Brazhkin V V, Popova S V. Met. Phys., 1985, 7: 103
- [13] Brixner L H. Mater. Res. Bull., 1972, 7: 879
- [14] Li D J, Wang J T, Ding B Z, Li S L. Chin. J. High Press. Phys., 1994, 8: 74
- [15] Li D J, Wang J T, Ding B Z, Qin Z C. Scr. Metall. Mater., 1993, 28: 1083
- [16] Hu Z Q, Guo W Q, Li D J, Jiang H G, Liu X D. Proc. Conf. C-MRS-94, Low-dimensional Materials. Beijing: Chem. Industry Press, 1995. 1
- [17] Li D J, Wang J T, Ding B Z. Scr. Metall. Mater., 1992, 26: 621
- [18] Liu H Z, Wang A M, Wang L H, Ding B Z, Hu Z Q. In: Liu B C, Jing T. Proceedings of the Third Pacific Rim International Conference on Modeling and Solidification Processes. New York: International Academic Publishers. 1996. 422
- [19] Yao B, Ding B Z, Sui G L, Wang A M, Hu Z Q. J. Mater. Res., 1996, 11: 912
- [20] Li D J, Wang A M, Yao B, Ding B Z, Hu Z Q. J. Mater. Res., 1996, 11: 2685
- [21] Li D J, Ding B Z, Yao B, Hu Z Q, Wang A M, Li S L, Wei W D. Nanostruct. Mater., 1994, 4: 323
- [22] Yao B, Li D J, Wang A M, Ding B Z, Li S L, Hu Z Q. Physica B, 1995, 212: 61
- [23] Liu H Z, Wang A M, Wang L H, Ding B Z, Hu Z Q. J. Mater. Sci. Lett., 1997, 16: 134
- [24] Liu H Z, Wang A M, Wang L H, Ding B Z, Hu Z Q. J. Mater. Res., 1997, 12: 1187
- [25] Li D J. PhD Thesis, Mechanism of phase transformation of metastable phases under high pressure. Institute of Metal Research, Chinese Academy of Sciences, 1993
- [26] Glazov V M, Koltsov V B. J. Phys. Chem., 1982, 55: 2759